Hindawi
Shock and Vibration
Volume 2019, Article ID 7572910, 17 pages
https://doi.org/10.1155/2019/7572910

Research Article

Analysis of the Occurrence Mechanism for Coal and Gas Outburst Based on Multiple Discriminant Indices

Hai Rong,[1,2] **Hongwei Zhang**,[1] **Bing Liang**,[2] **and Weihua Song**[1]

[1]*College of Mining, Liaoning Technical University, Fuxin, Liaoning Province, China*
[2]*School of Mechanics and Engineering, Liaoning Technical University, Fuxin, Liaoning Province, China*

Correspondence should be addressed to Hai Rong; ronghai1988@163.com

Received 9 May 2019; Revised 4 August 2019; Accepted 17 September 2019; Published 7 October 2019

Academic Editor: M. I. Herreros

In order to reveal the occurrence mechanism of coal and gas outburst and optimize the measures to prevent the disaster, a coal mine in Henan Province was undertaken as the research background. Based on the geological and mining conditions of the coal mine, the gas geological analysis method is applied to determine the outburst occurrence and to classify the risk levels. A multifactor pattern recognition method is used to determine the risk probability of the dynamic disasters such as coal and gas outburst. The relationship between geological structure, rock mass stress, and mine dynamic hazards is determined using geodynamic division method and FLAC^{3D} numerical simulation. The occurrence and manifestation characteristics of the dynamic hazards are determined. COMSOL Multiphysics software is used to evaluate the original prevention measures and to optimize the measures. The research results determine the main influencing factors and regional distribution law of coal and gas outburst, which is of great significance to the risk prediction and prevention of dynamic disasters such as coal and gas outburst.

1. Introduction

Coal and gas outburst is an instantaneously destructive geo-phenomenon caused by complex interactions among the gas, coal seam, rock mass, and ground stress [1, 2], which is also a typical dynamic disaster in coal mines. Many scholars have carried out numerous scientific research studies with regarding to the energy source and occurrence mechanisms of coal and gas outburst and achieved considerable research results. Yu and Shepherd et al. [3–5] think that geological structure is a prime factor in outburst occurrence. In addition, the outburst risk of the same coal mine and same coal seam at different locations is different, which is, namely, the regional distribution of outburst. Zhao [6] used numerical method to simulate the procedure of coal and gas outburst. Results show that the crushing level of the coal and rock depends on the outburst intensity. When the outburst is weak, the coal is only being squeezed out or dumped. Hu et al. [7] explored the mechanism of coal and gas outburst using theoretical analysis and numerical simulation. Results revealed that in the initial stage of coal and gas outburst, stress concentration occurred in surrounding rock mass and coal seam. In the development stage, surrounding coal around a borehole was of gradual failure. At the end of the outburst stage, the stress state of the coal around the borehole was changed. Miao et al. [8] studied the formation process of outburst shock wave by combination of the two-phase flow movement parameters of the coal and gas. It was considered that the velocity and intensity of the shock wave decreased with the increase of the fluid expansion in the roadway. Zhu and Fan et al. [9–14] took different methods to reveal the mechanism of coal and gas outburst. Sobczyk and Frid et al. [15–17] took different methods to forecast the risk of coal and gas outburst.

According to the characteristics of the coal and gas outburst in Xi'nan coalfield, Xu et al. [18] put forward several outburst prediction and controlling measures, including gas geology study, geological structure survey, gas predrainage, and coal seam permeability enhancement, introducing vibration blasting or long-distance blasting, and standardization of operational management.

To solve the problems of serious outburst and gas emission in No. 15 coal seam of Sijiazhuang Coal Mine, Liu et al. [19] put forward the technology of gas outburst prevention and controlling, including hydraulic fracturing, cross drilling, drilling while draining, and hydraulic forcing out of gas contents. Field tests showed good application results.

According to the management principle of "one mine one regulation, one panel one regulation" of Pingdingshan Coal Mine of Shenma Group, Zhang [20] has planned the outburst prevention and controlling key technologies, such as protection seam (nonburst seam) mining of multientry panel and extremely thin coal seam and high pressure hydraulic borehole. Zhang has developed a gas prevention and controlling system under consideration of local geological characteristics.

In coal and gas outburst study, scholars have carried out various preventive measures and considerable experiences. However, dynamic disasters such as coal and gas outburst are complex phenomena, and the occurrence mechanism and development characteristics of the disaster are not clear yet due to the complexity and diversity of geological conditions. With the deepening resource mining, the threat of dynamic disasters will become an important issue for mine safety.

In order to reveal the occurrence mechanism of coal and gas outburst, undertaking a coal mine in Henan Province as engineering background this paper compares 31020 burst working face with adjacent 17220 nonburst working face. Under considerations of the geological and mining conditions of the coal mine, the high risk outburst areas are determined using the gas geological analysis method, geological dynamic division method, multifactor pattern recognition method, and FLAC^{3D} numerical method, respectively. The geological and ground stress aspects related to coal and gas outburst are comparatively studied. The prevention measures in 31020 and 17220 working faces are analyzed using COMSOL Multiphysics software. The research results reveal the main influence factors and regional distribution of coal and gas outburst, which is of great significance to the risk prediction and prevention of coal and gas outburst.

2. Overview of the Panel

2.1. Overview of Panel 31020. Panel 31020 is located in the northern region of Guozhuang anticline in a coal mine, Henan Province, China. Panel 17220 is an adjacent panel of it to the north. The panel width of 31020 is 203 m, headgate length is 911 m, and tailgate length is 761 m. The coal seam is a simple structure and relatively stable, and the coal seam is 105°~130° in strike direction, which tends to the northeast. In the coal seam, the average inclination angle is 10°, the average thickness is 3.3 m, the initial gas pressure is 1 MPa, and the initial gas content is 14.97 m^3/t. Blasting method is used in the roadway excavation, with an average driving speed of 12 meters per day. The layout of the panel is shown in Figure 1. The lithology of the roof and floor of the panel is shown in Table 1.

The headgate excavation began from July 1st, 2017, the panel has not been mined at present. On November 25th, 2017, one coal and gas outburst accident occurred at 427 m, and total gas emission was 2458 m^3 and coal dump was 83 tons.

2.2. Overview of Panel 17220. Panel 17220 is located to the north of Panel 31020 with panel width of 158 m, panel length of 751.3 m, and mining height of 3.3 m.

The immediate roof of the panel is sandy mudstone with an average thickness of 4.01 m. The main roof is fine sandstone with an average thickness of 10.9 m. The immediate floor is mudstone with an average thickness of 0.3 m, and the main floor is argillaceous sandstone, with an average thickness of 6.8 m. Before Panel 17220 being mined, the maximum original gas pressure was 2.6 MPa, the original gas content was 15.256 m^3/t, and the absolute gas emission was 4.31 m^3/min. A comprehensive mechanized mining method was adopted for mining. The average mining speed was 2.4 m/d using the full roof caving method. The geological structure of the panel is simple. In the mining area, there are only two small faults, with the throw between 0.2 m and 0.5 m. A 36U-steel arch shed was used for the inlet roadway support, and outlet roadway was supported by a bolt and mesh.

3. Prediction Results of Coal and Gas Outburst Risk in Panel 31020

3.1. Prediction Results of Gas Geological Map. According to Cluster 200 in Chinese Coal Mine Safety Regulations 2016, gas geological maps in a coal and gas outburst mine must be compiled and updated in time, and the renewal period should be less than one year. In the gas geological maps, the mining progress, the protecting area, conditions of coal seam, geological structure, location of outburst points, strength of outburst and basic parameters of gas, etc. should be indicated clearly, which is used as a base line for coal and gas outburst prediction and prevention.

According to the gas geological map of the mine updated in September 2018, high risk outburst region was the northern region of Guozhuang anticline with floor contour greater than −350 m (overlying strata thickness more than 430 m).

Floor contour of Panel 31020 is from −630 m to −696 m, and the depth of the panel is from 880 m to 976 m, both conditions have reached the critical state of the outburst risk. Prediction results of Panel 31020 by gas geological map are shown in Figure 2.

Panel 17220 is located in the northern region of Guozhuang anticline. Floor contour is −560 m to −610 m, and the depth of the panel is 750 m to 800 m. It indicated that risk of coal and gas outburst also exists in Panel 17220. Prediction results of Panel 17220 by gas geological map are shown in Figure 3.

3.2. Research Results of Geo-Dynamic Division. Geo-dynamic division method evaluates tectonic activities and effects at 5 different scales, from I to V. Level-I

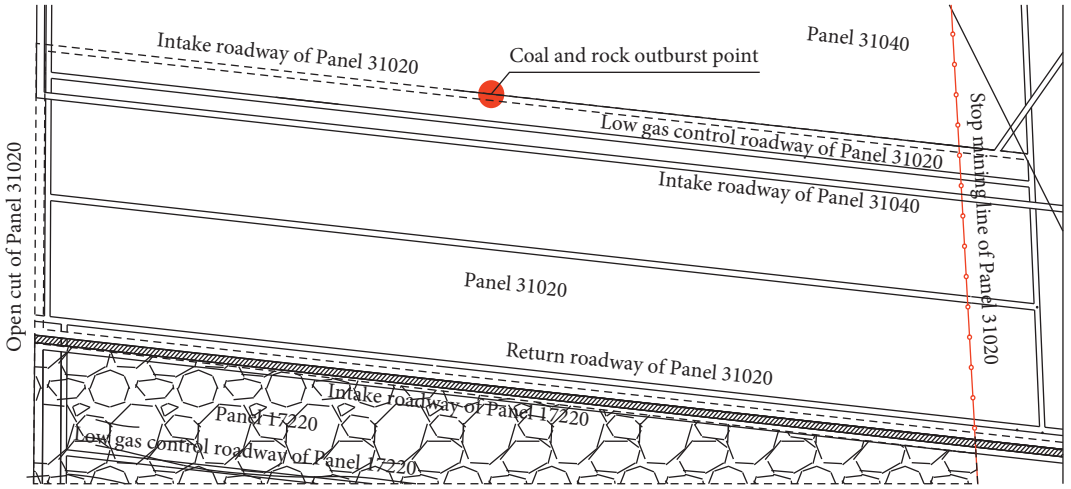

Figure 1: Layout of the Panel 31020 in a coal mine in Henan Province.

Table 1: Lithology and thickness of the roof and floor of Panel 31020.

Name	Lithology	Feature description	Thickness
Main roof	Fine sandstone	Gray fine sandstone with a small number of patches at the top, sandy mudstone, mica sheets, and strips at the middle and lower parts	10.9 m
Immediate roof	Sandy mudstone	Gray-black sandy mudstone, dense, mica-bearing fragments	4.01 m
Immediate floor	Mudstone	Gray mudstone	0.3 m
Main floor	Sandy mudstone	Gray sandy mudstone, massive	1.5 m~12 m

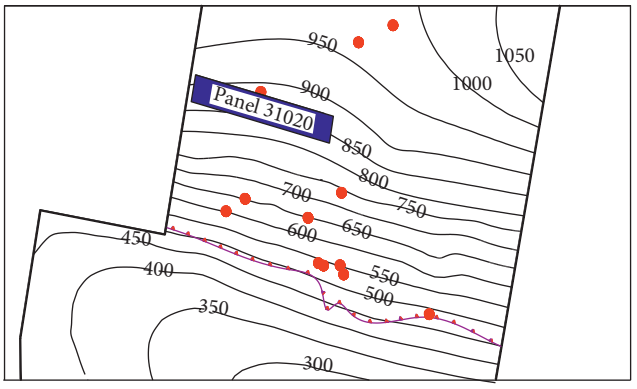

Figure 2: Prediction results of Panel 31020 by gas geological map.

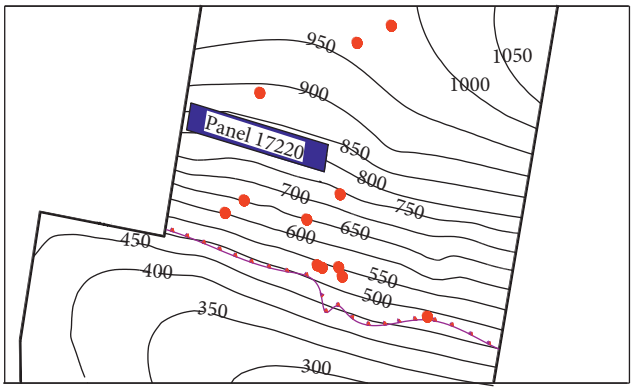

Figure 3: Prediction results of Panel 17220 by gas geological map.

establishes the relationship between tectonic effect and regional geological structure. The next level division refines the research contents and narrows the regional scope than the previous level division. The level-V division corresponds to the scope of the coal mine field (as shown in Figure 4). Through systematic regionalization, the relationship between tectonic effect and engineering application can be established. The geological structure and geo-dynamic background of the engineering project are then determined. After the boundary of tectonic fault blocks of all levels is identified, the tectonic active areas are divided and the geological structure model of the engineering location can be established. Finally, the stress state of the rock mass is analyzed, and the risk levels of coal and gas outburst are divided. After the risk of coal and gas outburst is predicted, the geological dynamic effect produced by engineering activities is finally achieved.

The scale of level I and II blocks ranges from 1 : 2.5 million to 1 : 1 million. Geo-dynamic division determines the relationship between plate tectonic division and geo-dynamic division, and then applies the theories and research results developed from plate tectonics to the geo-dynamic region. The scale of level III and IV blocks ranges from 1 : 200,000 to 1 : 25,000. Accordingly, the block structure could be used in a coalfield scale. The level-V block is in the scale of 1 : 10,000, which can be further reduced to a coal mine.

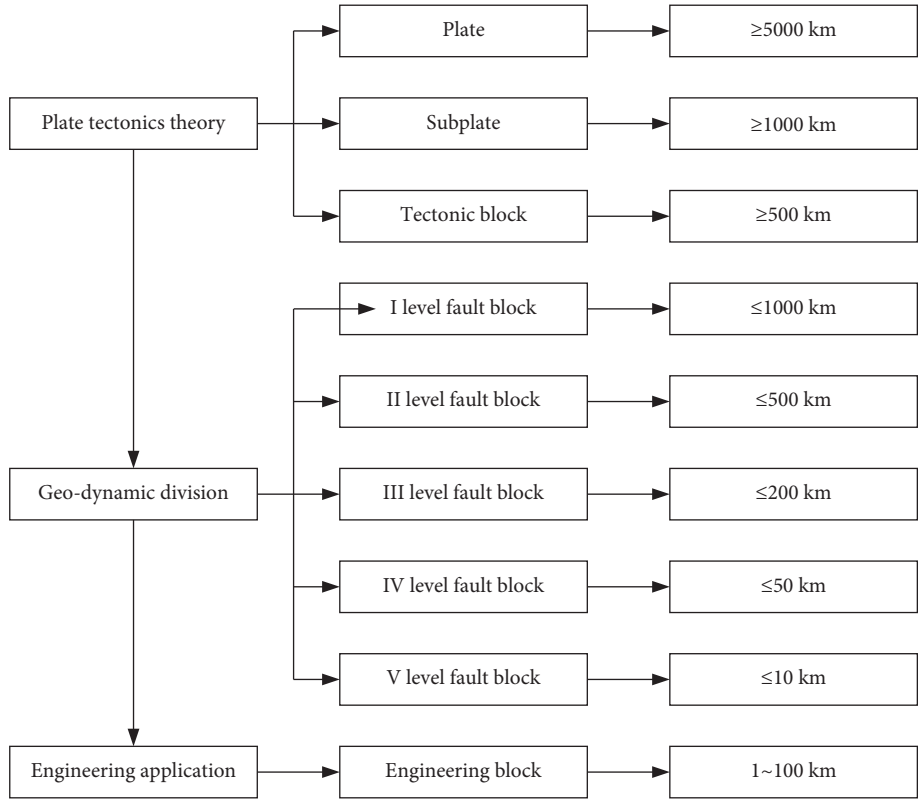

Figure 4: Relationship between geo-dynamic division and tectonic and engineering application.

Through the process of regionalization from 1 : 25 million to 1 : 10,000, the block structure in the coal mine can be determined, and the relationship between local structure and engineering project is finally established.

The geo-dynamic division method is used to divide level I–V blocks of this coal mine. The distribution of active faults and coal and gas outburst risk levels are shown in Figure 5. Of all 12 coal and gas outbursts occurred in the coal seam, 11 of them occurred near level III and V division faults, five occurred near level III-12 faults, four occurred near level V-12 and V-25 faults, one occurred near level V-14 faults, and one occurred near the intersection of V-13, V-23, and V-24 faults. The faults in the geo-dynamic division are located at the junction in the northern part of the Guozhuang anticline and southern part of the Likou syncline. Their distribution direction is similar to that of the Likou syncline and the Guozhuang anticline, which are closely related to the geological structure between the southern part of the Likou syncline and northern part of Guozhuang anticline.

According to the distribution of the fault structure and outburst points, level III faults control the coal and gas outburst in the mining field. Within the influence of level III faults, most of the outbursts occur in the vicinity of level V faults or in dense fault area.

Among them, the outburst accident on November 25th, 2017, occurred at the intersection of V-13 fault and inlet roadway of Panel 31020. It was 172 m away from the intersection of V-13, V-23, and V-24 fault. Therefore, it could be concluded that the occurrence of the coal and gas outburst was related to the geo-dynamic division fractures, and the outburst was affected by V-13, V-23, and V-24 fault. Coal and rock mass at the fault intersection were seriously damaged, which provided the condition for energy release in coal and gas outburst. Based on the geo-dynamic division method, the dynamic hazard risk prediction results of Panel 31020 are shown in Figure 6.

According to the results of the geo-dynamic division method, only two small faults with a throw of 0.2 m and 0.5 m were exposed during the excavation and mining of Panel 17220, and only V-24 division fault was found in the panel, which had small impact on the dynamic disasters of coal and gas outburst.

3.3. Multifactor Pattern Recognition Method. Multifactor pattern recognition method can be used to analyze multiple influencing factors and patterns of coal and gas outburst. By dividing the prediction units in the study area, the probability based prediction of subunit pattern recognition can be realized, which promotes the prediction from a point to the regional prediction, from single factor prediction to multifactor prediction, and from qualitative prediction to quantitative prediction.

The multifactor pattern recognition method is used to evaluate the risk of coal and gas outburst on November 25th, 2017. By comparing the single factor on the outburst risk, it could be found that the dangerous area mainly distribute in the high stress area and high stress gradient area. The maximum stress in the high stress area was located in the north of the mining field, and the maximum principal stress

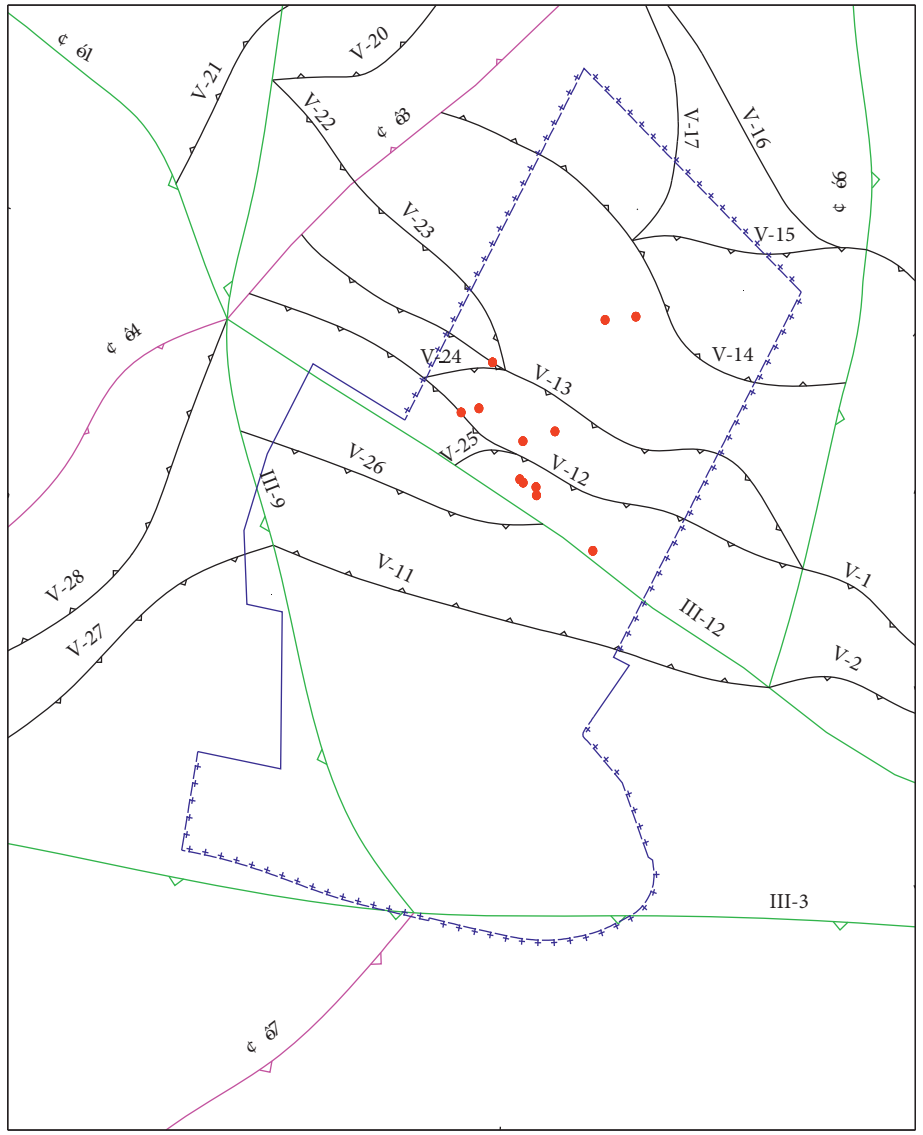

Figure 5: The distribution of active faults and coal and gas outbursts.

was 39 MPa. The minimum stress was located in the south of the mining field, and the minimum principal stress was 28 MPa. The maximum and minimum probability of outburst risk of the coal seam was 0.99 and 0.15. The mining field was divided into five levels, and the critical value of the risk was 0.34, 0.58, 0.78, and 0.84.

The prediction results for Panel 31020 by the multifactor pattern recognition method are shown in Figure 7. The probability of coal and gas outburst in the area of Panel 31020 was 0.95, which was higher than 0.84. According to the result of risk classification of outburst, it shows high outburst risk existed in Panel 31020.

According to the prediction results of gas geological map and multifactor pattern recognition, outburst risk existed in Panel 31020.

According to the prediction result of multifactor pattern recognition, the probability of coal and gas outburst in Panel 17220 is 0.90–0.95, and high outburst risk also existed in Panel 17220, as shown in Figure 8.

4. Influence of Roadway Development to Panel Face Stress Distribution

4.1. Stress Distribution of Panel 31020 in Roadway Development Process. The position of Panel 31020 and Panel 17220 is shown in Figure 9. To study the stress distribution in the development process of the intake roadway, a numerical model is established using FLAC^{3D} software. The size of the model is 900 m × 550 m × 120 m, and a total of 738970 elements and 784958 nodes are established (as shown in Figure 10).

The boundary conditions of the model are determined as follows:

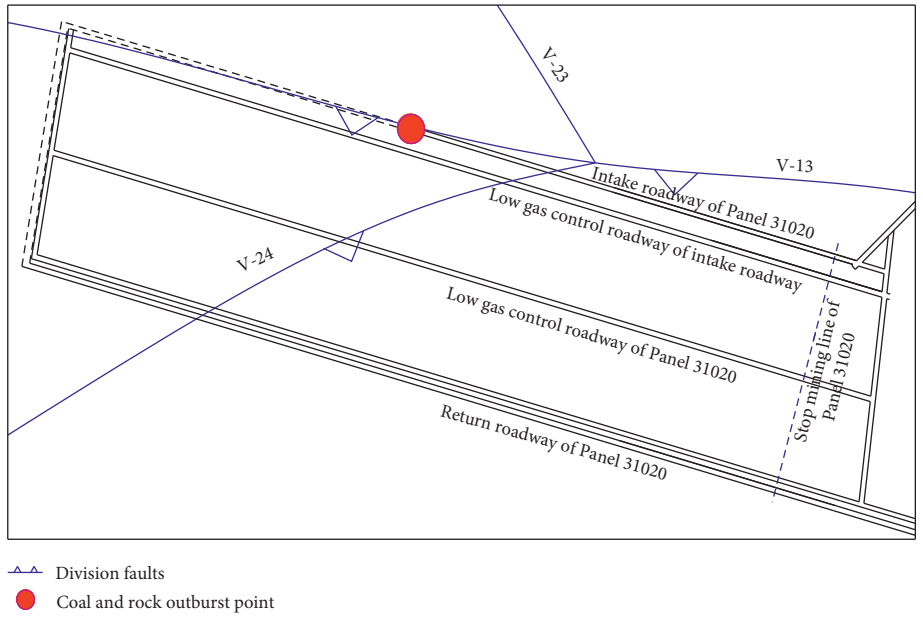

Figure 6: Dynamic hazard risk prediction results of Panel 31020 based on the geo-dynamic division method.

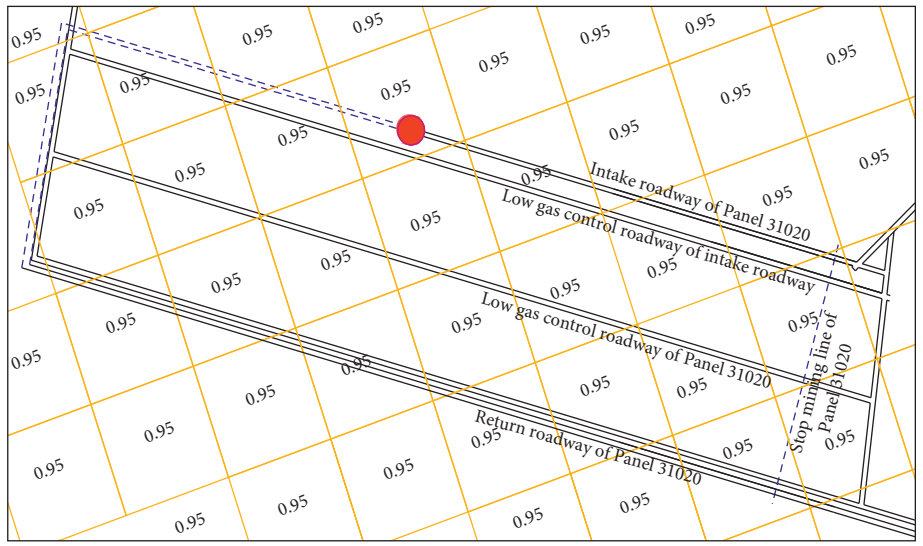

Figure 7: Prediction results for Panel 31020 by the multifactor pattern recognition method.

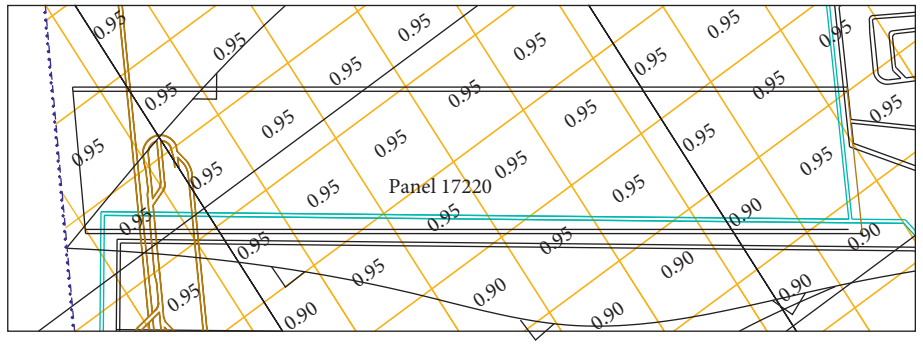

Figure 8: Prediction results for Panel 17220 by the multifactor pattern recognition method.

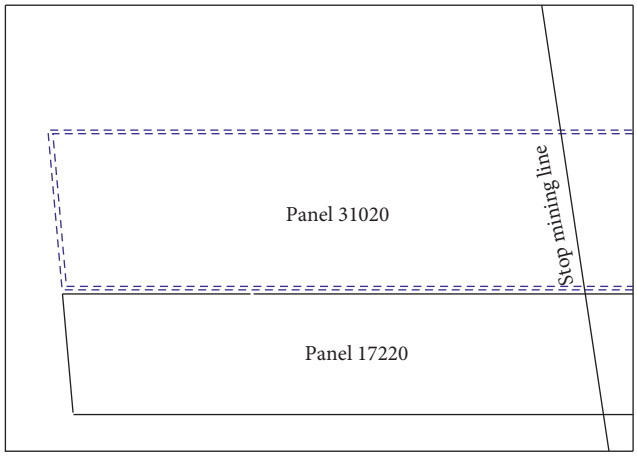

Figure 9: Panel 31020 and Panel 17220.

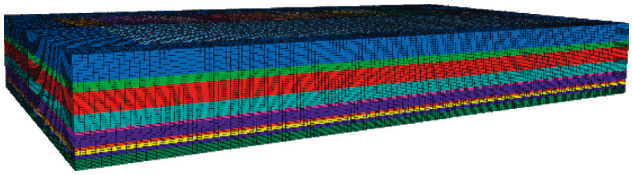

Figure 10: Numerical model of the panel.

(1) The boundary of the x-axis of the model is constrained along the x-axis, and the displacement of the X-direction of the boundary is zero

(2) The boundary of the y-axis of the model is constrained along the y-axis, and the displacement of the Y direction of the boundary is zero

(3) The bottom boundary of the model is fixed, and the displacements in X, Y, and Z directions of the bottom boundary are all zero

Based on the results of in situ stress measurement in the mine, the boundary load conditions of the calculation model are as follows:

(1) The gradient stress of 25 MPa to 28.8 MPa is applied to the x-axis direction of the model

(2) The gradient stress of 15.6 MPa to 18.0 MPa is applied to the y-axis direction of the model

(3) The gradient stress of 19.5 MPa to 22.5 MPa is applied in the z-axis direction of the model, the equivalent load of 19.5 MPa is applied in the upper part of the model, and the self-weight load is set in the z-axis direction

The mechanical parameters of coal and rock used in this simulation work are shown in Table 2.

The original rock stress of the intake roadway of Panel 31020 is 22.0 MPa. When the intake roadway is excavated 100 m, the surrounding rock stress of the roadway reaches 27.2 MPa and the stress concentration factor is 1.24. When the intake roadway is excavated 200 m, the surrounding rock stress of the roadway reaches 27.5 MPa and the stress concentration factor is 1.25. With the continuous excavation of the intake tunnel, the stress of surrounding rock tends to be stable. The vertical stress distribution of surrounding rock in two roadways of Panel 31020 is shown in Figure 11.

In summary, during the excavation of Panel 31020 intake roadway, the stress concentration factor is between 1.24 and 1.25. The stress of the coal and rock mass increases by 24%-25% during the excavation of the roadway, which increases the risk of dynamic disasters such as coal and gas outburst.

4.2. Stress Distribution of Panel 17220 in Mining Process

4.2.1. Stress Distribution during Panel 17220 Retreat. According to the position of Panel 17220, a numerical model is established by FLAC^{3D} software to study the stress distribution in the mining process. The size of the model is 920 m × 520 m × 120 m, a total of 648960 elements and 68399 nodes are established (as shown in Figure 12).

Based on the in situ stress measurement in the mine, the boundary load conditions of the calculation model are as follows:

(1) The gradient stress of 23.4 MPa to 27.2 MPa is applied to the x-axis direction of the model

(2) The gradient stress of 14.6 MPa to 17.0 MPa is applied to the y-axis direction of the model

(3) The gradient stress of 18.25 MPa to 21.25 MPa is applied in the z-axis direction of the model, the equivalent load of 18.25 MPa is applied in the upper part of the model, and the self-weight load is set in the z-axis direction

The stress in Panel 17220 is high along return roadway but is low along intake roadway. The stress on the intake roadway side of Panel 17220 is 20.25 MPa, which is the original stress. Under the influence of the lateral abutment pressure near the goaf, the stress on the return air roadway side of Panel 17220 reaches 40 MPa, and the stress concentration factor is 1.98.

The stress distribution of coal and rock mass of Panel 17220 when the maingate is excavated 200 m is shown in Figure 13. When the intake roadway of Panel 17220 is excavated 100 m, the stress of surrounding rock of the roadway reaches 24.2 MPa and the stress concentration factor is 1.2. When the intake roadway of Panel 17220 is excavated 200 m, the stress of surrounding rock of the roadway reaches 24.4 MPa and the stress concentration factor is 1.2. When the intake roadway of Panel 17220 is drived 300 m, the stress of surrounding rock of the roadway reaches 24.4 MPa and the stress concentration factor is 1.2. With the continuous excavation of the intake tunnel, the stress of surrounding rock tends to be stable.

When the tailgate of Panel 17220 is excavated 100 m, the stress of surrounding rock reaches 42.1 MPa and the stress concentration factor is 2.08. When the tailgate is excavated 200 m, the stress of surrounding rock reaches 42.4 MPa and the stress concentration factor is 2.09. When the tailgate is drived 300 m, the stress of surrounding rock reaches 43.3 MPa and the stress concentration factor is 2.14. With

Table 2: Mechanical parameters of coal and rock.

Coal and rock	Density (kg·m^{-3})	Bulk modulus (GPa)	Shear modulus (GPa)	Internal friction angle (°)	Cohesion (MPa)	Tensile strength (MPa)
Fine sandstone	2600	37.4	26.9	45	15.4	7.8
Limestone	2650	30.4	16.5	38	14.6	7.3
Coal	1410	14.8	6.06	25	2.1	1.8
Mudstone	2400	23.3	10.8	28	3.7	2.8
Sandy mudstone	2400	24.2	12.5	46	6.8	4.1
Medium grain sandstone	2400	34	21.4	36	13.4	6.5

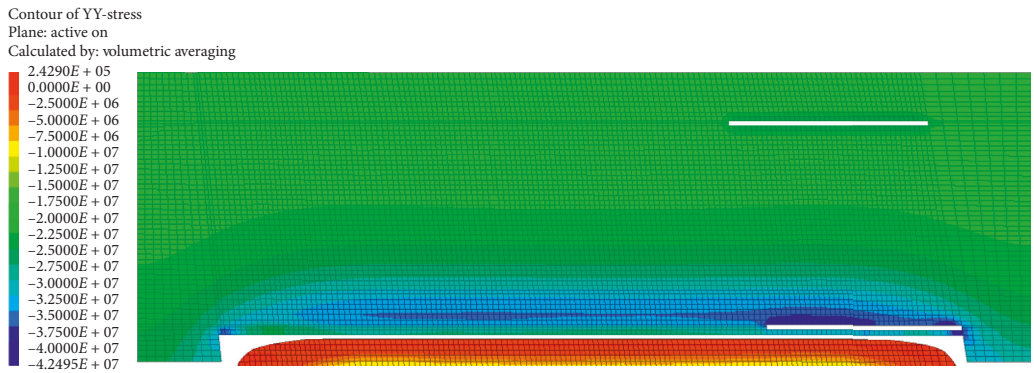

Figure 11: The vertical stress distribution of surrounding rock in two roadways of Panel 31020.

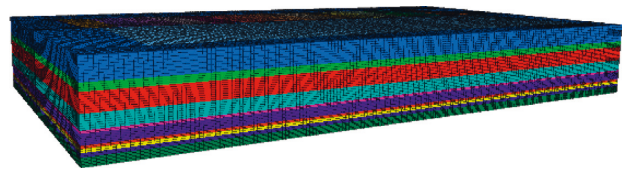

Figure 12: Numerical model of Panel 17220.

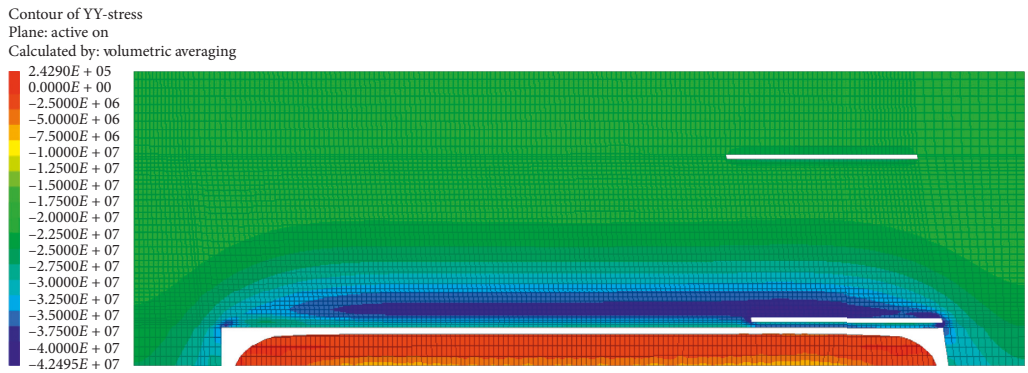

Figure 13: The stress distribution of coal and rock mass of Panel 17220 when maingate is excavated 200 m.

the continuous excavation, the stress of surrounding rock tends to be stable.

In summary, during the excavation of Panel 17220, the stress concentration factor of the intake roadway is 1.20 and the stress concentration factor of the return roadway is 2.08–2.14. With the continuous excavation, the stress of surrounding rock tends to be stable.

4.2.2. Stress Distribution during Mining Process of Panel 17220. The stress distribution in the mining process of Panel 17220 is shown in Figures 14–16. In the process of mining, the concentration of advanced abutment pressure is not high in the intake roadway of the panel, but is significant along the return roadway of the panel. When Panel 17220 is mining 100 m, the peak value of advance abutment pressure

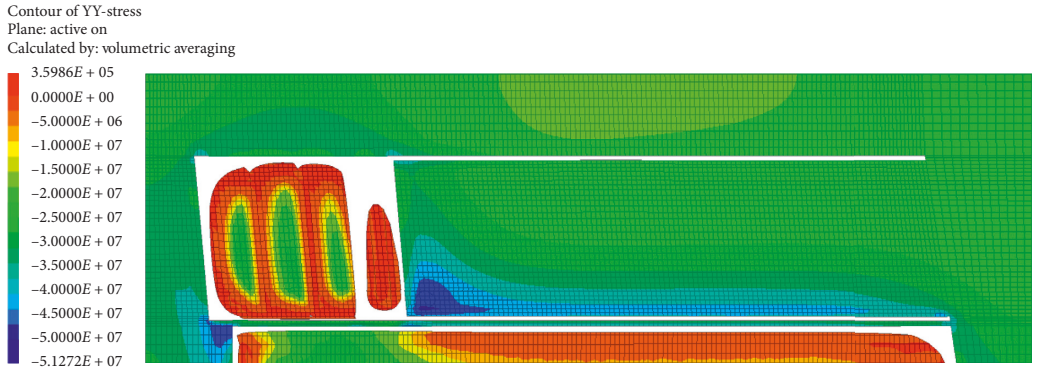

Figure 14: The stress distribution of coal and rock mass of Panel 17220 when retreat 200 m.

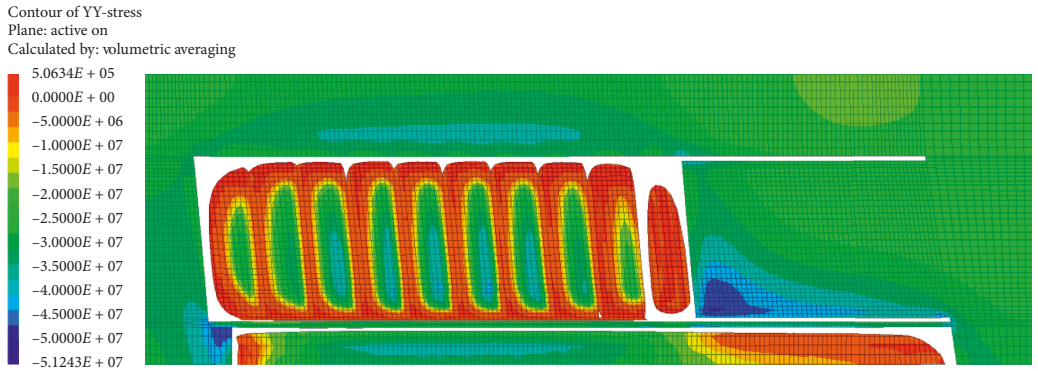

Figure 15: The stress distribution of coal and rock mass of Panel 17220 when retreat 500 m.

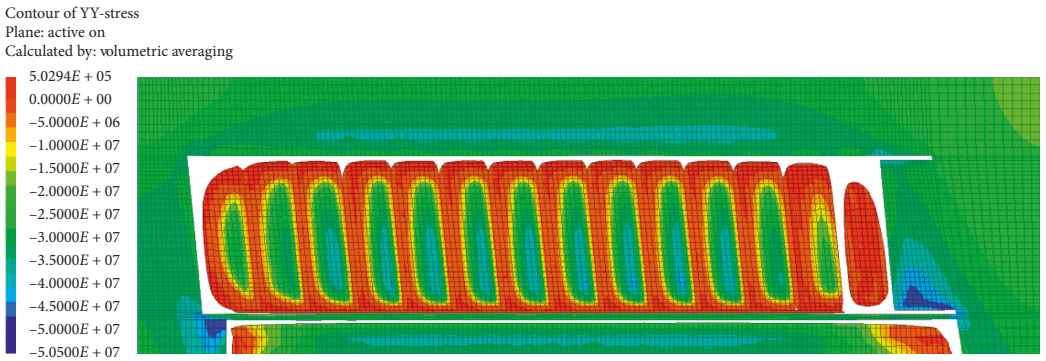

Figure 16: The stress distribution of coal and rock mass of Panel 17220 when retreat 700 m.

is 47.9 MPa, the stress concentration factor is 2.37, the peak point is 20 m in front of the face, and the influence range of advance abutment pressure is 80 m. When mining 200 m, the peak advance abutment pressure is 51.2 MPa, the stress concentration factor is 2.53, the peak point is 20 m ahead of the coal, and the influence range of the advance abutment pressure is 85 m. When mining 300 m, the peak advance abutment pressure is 51.2 MPa, the stress concentration factor is 2.53, the peak point is 20 m ahead of the coal, and the influence range of the advance abutment pressure is 85 m. With the continuous mining of the panel, the stress of surrounding rock tends to be stable.

In summary, in the mining process of Panel 17220, the peak advance abutment pressure is from 47.9 MPa to 51.2 MPa, the stress concentration coefficient is 2.37–2.53, the peak point is 20 m ahead of the working face, and the influence range of advance abutment pressure is 80 m–85 m.

5. Study of Measures to Minimize Risk

5.1. Mathematical Model of Gas Drainage

5.1.1. Seepage Field Equation. The gas migration in coal seam follows Darcy's law:

$$\frac{\partial m}{\partial t} + \nabla \cdot \left(\rho_g \overrightarrow{u}\right) = Q_s. \tag{1}$$

The gas quality per unit volume is as follows:

$$m = \rho_g \varphi + \rho_{gs} \rho_c \frac{V_L p}{p_L + p}. \tag{2}$$

According to Darcy's law, considering the Klingberg effect in gas migration, the velocity of gas migration in fissures is as follows:

$$\overrightarrow{u} = -\frac{k}{\mu_g}\left(1 + \frac{b}{p}\right)\nabla p. \tag{3}$$

By substituting formula (2) and formula (3) into formula (1), it can be concluded that

$$\frac{\partial}{\partial t}\left(\rho_g \varphi + \rho_{gs} \rho_c \frac{V_L p}{p_L + p}\right) + \nabla \cdot \left(-\frac{\rho_g k}{\mu_g}\left(1 + \frac{b}{p}\right)\nabla p\right) = 0. \tag{4}$$

Formula (4) is the equation of gas seepage field in gas-bearing coal seam.

5.1.2. Stress Field Equation. The stress variation of coal body is influenced by in situ stress, gas pressure, and gas adsorption/desorption. Then, the stress-strain relationship of coal satisfies.

$$\varepsilon_{ij} = \frac{1}{2G}\sigma_{ij} - \left(\frac{1}{6G} - \frac{1}{9K}\right)\sigma_{kk}\delta_{ij} + \frac{\alpha p}{3K}\delta_{ij} + \frac{\varepsilon_a}{3}\delta_{ij}. \tag{5}$$

Among them,

$$\begin{cases} G = \dfrac{D}{2}(1 + \nu), \\ K = \dfrac{E}{3}(1 - 2\nu), \\ K_s = \dfrac{E_s}{3}(1 - 2\nu), \\ \alpha = 1 - \dfrac{K}{K_s}. \end{cases} \tag{6}$$

5.1.3. Coupling Relationship. In the process of gas extraction, the stress change and gas migration are after changing the porosity and permeability of the coal body. Porosity and permeability, as key parameters of gas extraction in coal seam, are affected by deformation stress field and seepage field of gas migration. Therefore, the porosity in coal can be described as

$$\varphi = \varphi_0 - \frac{3\varphi_0}{\varphi_0 + 3L_f/K}\left(\frac{\varepsilon_L \Delta p}{p_L + \Delta p} - \varepsilon_v\right). \tag{7}$$

According to the relationship between permeability and porosity of coal seam, it can be concluded that

$$k = k_0\left(1 - \frac{3}{\varphi_0 + 3L_f/K}\left(\frac{\varepsilon_L \Delta p}{p_L + \Delta p} - \varepsilon_v\right)\right)^3. \tag{8}$$

Formulas (4)–(8) are combined to form a gas-solid coupling model for gas extraction. The numerical simulation of gas extraction can be carried out by a solid mechanics module and a PDE module in COMSOL Multiphysics simulation software, and the effect of gas extraction in coal seam can be analyzed.

5.2. Analysis of Gas Drainage Effect in Intake Roadway of Panel 31020

5.2.1. Analysis of Original Extraction Scheme in Intake Roadway of Panel 31020

(1) Physical Model and Simulation Scheme. The original design started from the stopping line of the gas control roadway 20 m outward, drilling a group of boreholes with 6 m interval in the coal seam where the intake roadway was located. Each group of boreholes is designed with 9 diameter of 89 mm boreholes. The control range of boreholes is 15 m out of the two sides of the intake roadway, and the depth of boreholes is 0.5 m in the roof. There are 127 groups of boreholes in the design, totaling 1524 holes. From July 8th, 2016, to May 10th, 2017, 1143 predrainage boreholes were drilled through the gas control roadway of Panel 17220, with a cumulative hole length of 38,290 m, as shown in Figure 17.

According to the gas extraction scheme in intake roadway of Panel 31020, the numerical calculation model is established by COMSOL Multiphysics software, and gas extraction effect and gas migration characteristics of intake roadway are calculated. The size of the model is 125 m × 60 m × 45 m, as shown in Figure 18, and the parameters used in the simulation are shown in Table 3.

According to the FLAC^{3D} stress analysis of the intake roadway in Panel 31020, the stress concentration factor of the intake roadway is 1.25. Therefore, two sets of simulation schemes with stress concentration factor 1.00 and 1.25 are designed so as to study the effect of stress concentration on gas extraction. The simulation duration is 270 days.

(2) Boundary Conditions. Borehole boundary is the negative pressure of extraction, and the negative pressure of extraction is determined by the equipment parameters and extraction capacity of the coal mine. Because of the low permeability of coal seam roof and floor, they are set as the impermeable boundary. In the boundary of coal seam, the influence range of borehole is limited, which has little influence on the result.

The boundary conditions of the model are as follows: the bottom of the model is a fixed boundary, the periphery is a sliding boundary, and the boundary between coal seam and rock seam is a gas impermeable boundary. The top of the model is subjected to the gravity of overburden, and the surrounding model is subjected to the horizontal stress. The boundary of the extraction borehole is set as the Dirichlet boundary condition.

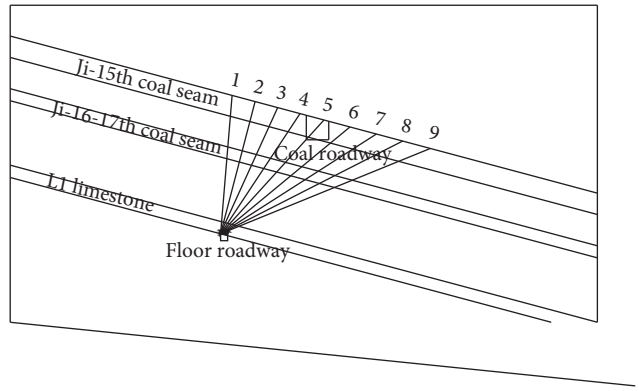

Figure 17: Layout of gas drainage borehole in intake roadway of Panel 31020.

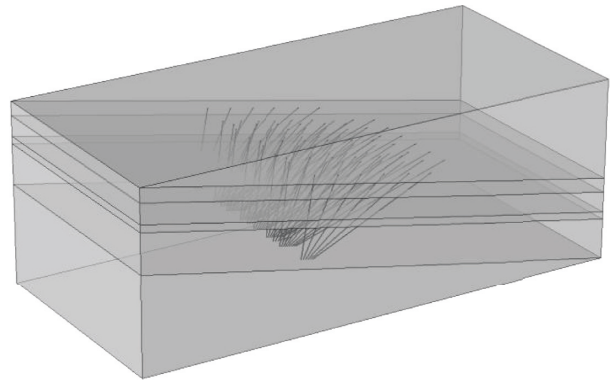

Figure 18: Geometric model of gas drainage in intake roadway of Panel 31020.

Table 3: Parameters for simulation.

Parameter	Porosity φ_0	Adsorption constant a	Adsorption constant b	Permeability k_0	Slippage factor h	Modulus of elasticity E	Poisson ratio ν
Value	0.035	26.615 m^3/t	0.568 MPa^{-1}	0.018 mD	0.76 MPa	3.75 GPa	0.25

Combining with the test results of in situ stress and gas extraction in this mine, the boundary load conditions imposed by the model are as follows: 22β MPa is applied on the top of the model, 35β MPa is applied in the X direction of the model, self-weight load is applied on both coal seam and rock seam, and 41 kPa negative pressure is applied on the boundary of the extraction borehole.

(3) Analysis of Simulation Results. The Henan Provisional Provisions for Enhancing Safety in Production of Coal Mines in 2014 stipulates that when the gas pressure in the coal seam is greater than 0.6 MPa or the gas content in the coal seam is greater than 6 m^3/t, the coal seam gas must be predrained by protective mining or bottom (top) slate roadway, and it is strictly forbidden to adopt local outburst prevention measures instead of regional outburst prevention measures. The residual gas pressure and gas content must be reduced to less than 0.6 MPa and 6 m^3/t before mining.

Figure 19 shows gas pressure nephograms with different stress coefficients. It could be seen from the graph that when the stress coefficient is 1.0, a low gas pressure zone is formed near the borehole after gas drainage for 270 days, and the gas pressure in the area decreases to 0.4 MPa~0.65 MPa. When the pressure coefficient is 1.25, the gas pressure is similar to that at 1.0.

After gas drainage for 270 days, when the stress coefficient is 1.00, the peak gas pressure is 0.62 MPa~0.63 MPa, which decreases by 37%~38% compared with the initial gas pressure. When the stress coefficient is 1.25, the peak gas pressure is 0.63 MPa~0.64 MPa, which decreases by 1.59%~1.61%, as shown in Figure 20.

Gas pressure around outburst point with different stress concentration factors is shown in Figure 21. After gas drainage for 270 days, five peak gas content points form. When the stress coefficient was 1.00 and 1.25, the peak gas content was 6.93 m^3/t to 7.00 m^3/t and 7.06 m^3/t to 7.12 m^3/t, respectively. Compared with the initial gas content, the decrease ranges were 53.58% and 52.71%, respectively.

According to the simulation results, the original extraction scheme of intake roadway in Panel 31020 does not meet the relevant requirements of outburst prevention and control in Henan Province, as the peak gas pressure of

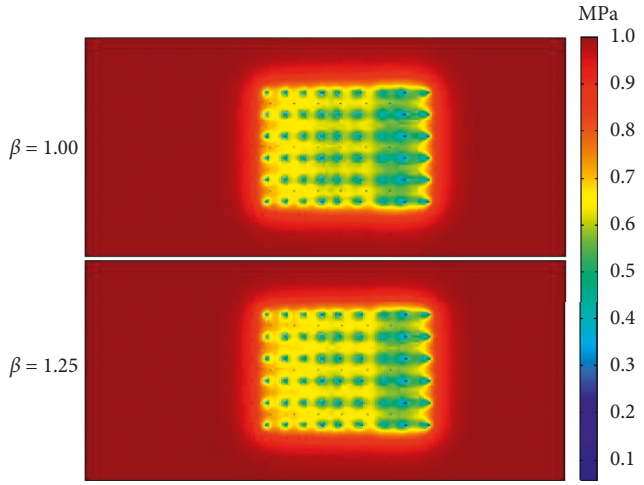

Figure 19: Gas pressure nephograms with different stress coefficients.

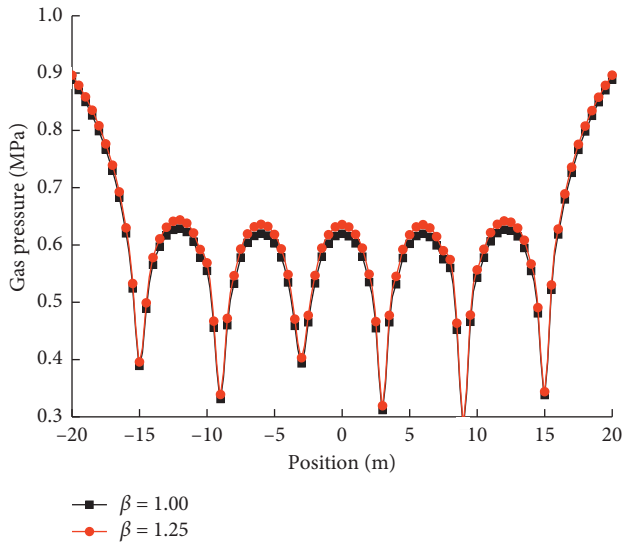

Figure 20: Gas pressure distribution around outburst points with different stress coefficient.

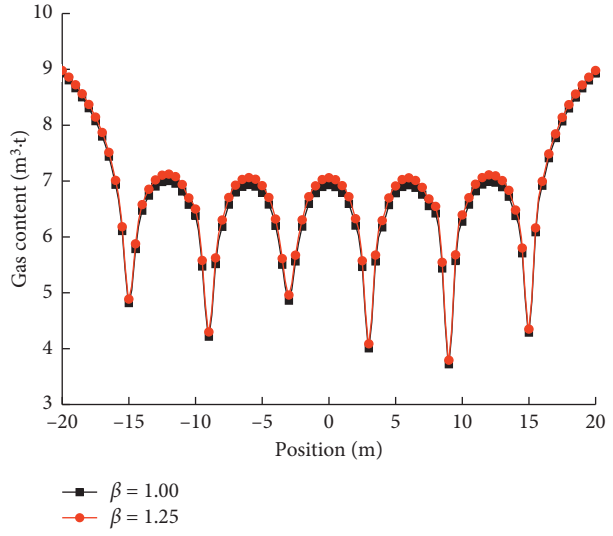

Figure 21: Gas pressure distribution around outburst point with different content coefficient.

0.63 MPa and 0.64 MPa are higher than the required index of 0.6 MPa, and the peak gas content of 7.00 m^3/t and 7.12 m^3/t are higher than the required index of 6 m^3/t.

5.2.2. Analysis of Second Gas Drainage in Intake Roadway

(1) Filling Scheme. On the basis of the original model, a group of 6 boreholes of diameter 89 mm are drilled every 12 m. The gas extraction with extra boreholes is simulated for further 180 days on the basis of the original simulation. According to the simulation results, the stress concentration factor has a great influence on the effect of gas drainage. In order to simulate the engineering reality and simplify the simulation process, only one group of gas drainage scheme with stress concentration factor of 1.25 are set up in the simulation scheme. The gas drainage after secondary borehole drilling is analyzed when the stress concentration factor is 1.25. The boundary conditions are the same as the original boundary conditions, and the borehole boundary after extra holes is set as the Dirichlet boundary condition, and the negative pressure of extraction is applied.

(2) Analysis of Simulation Results. Figure 22 shows gas pressure nephogram after second drainage. After gas drainaging for further 180 days, a distinct low-pressure area is formed in the simulated area, and the gas pressure decreased to 0.1 MPa~0.5 MPa, which was 23%~75% lower than that of the original simulation scheme. At this time, eight peak gas pressure points are formed around the stress concentrated outburst point, and the pressure values are 0.39 MPa~0.51 MPa (as shown in Figure 23). Compared with the original simulation scheme, the peak gas pressure decreases by 20.31%~38.1%. The gas pressure can meet the requirements of outburst prevention and control in Henan Province, China.

Distribution of gas content around stress coefficient outburst point is shown in Figure 24. After gas drainaging for 180 days, the peak gas content is from 4.86 m^3/t to 5.14 m^3/t, which is 31.16% lower than that of the original simulation scheme. The gas content can satisfy the qualified index that the residual gas content should not exceed 6 m^3/t in Henan Province, China.

5.2.3. Validity of the Proposed Measures in Intake Roadway of Panel 31020.

A group of test boreholes are drilled every 50 m from the opening of the intake roadway. There are 10 groups with 2 holes in each group at 75 mm diameter. Residual gas content and residual gas pressure are measured in each hole. The results of gas pressure and gas content in intake roadway of Panel 31020 are shown in Table 4 and Figures 25 and 26.

After supplementary drilling, the residual gas pressure decreases to 0.25 MPa~0.5 MPa, less than 0.6 MPa, and the residual gas content decreases to 4.1869 m^3/t~5.6859 m^3/t, less than 6 m^3/t, which conforms to the relevant regulations of Henan Province. It shows that the measures are effective.

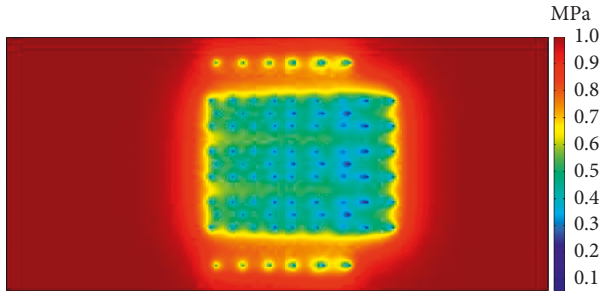

Figure 22: Gas pressure nephogram after second drainage.

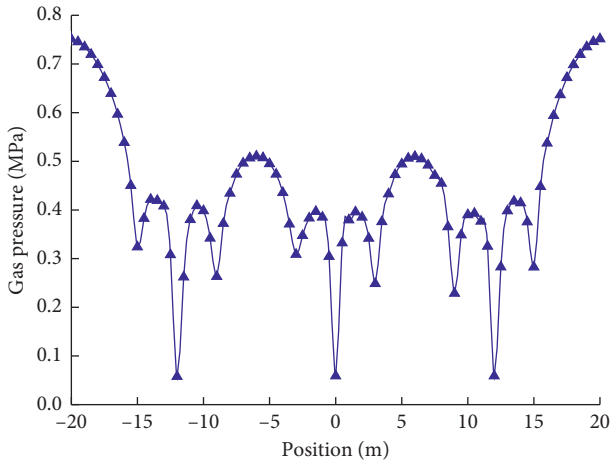

Figure 23: Gas pressure around outburst point.

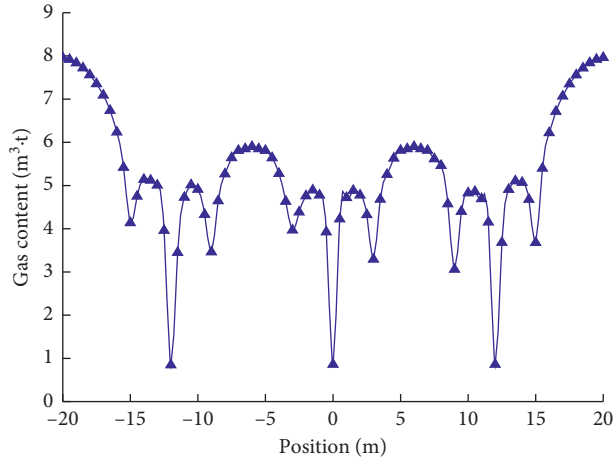

Figure 24: Distribution of gas content around outburst point.

5.3. Analysis of Gas Drainage Effect in Intake Roadway of Panel 17220

5.3.1. Simulation Scheme. According to the gas extraction scheme in intake roadway of Panel 31020, the numerical model is established by COMSOL Multiphysics software, and gas extraction effect and gas migration characteristics of intake roadway are studied. The size of the model is 100 m × 150 m × 3.3 m, as shown in Figure 27, and the

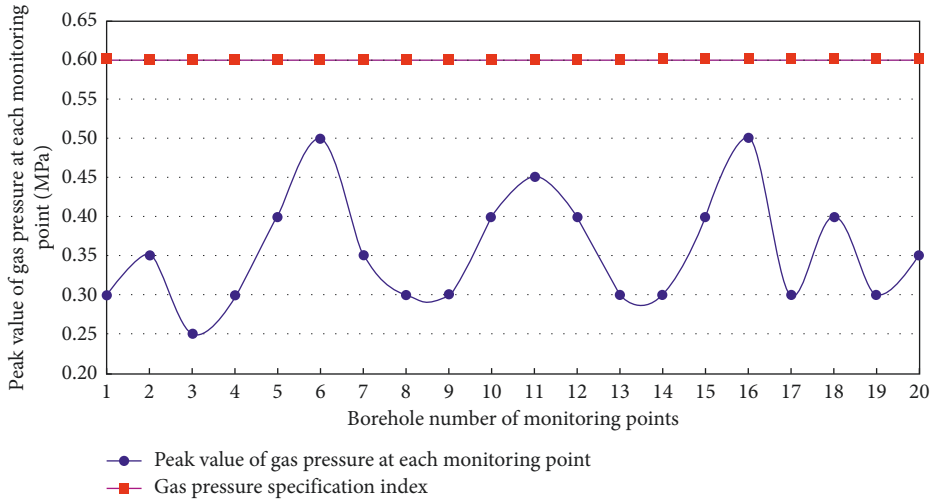

Figure 25: Gas pressure of inlet roadway in Panel 31020.

Table 4: Gas pressure and gas content in inlet roadway of Panel 31020.

Drilling position	Drilling number	Measuring point depth (m)	Measuring point elevation (m)	Peak pressure (MPa)	Gas content ($m^3 \cdot t^{-1}$)
50 m inward opening of low control roadway	1	904	−654	0.30	5.0667
	2	904	−654	0.35	4.7032
100 m inward opening of low control roadway	3	906	−656	0.25	4.8338
	4	906	−656	0.30	4.1869
150 m inward opening of low control roadway	5	909	−659	0.40	5.4853
	6	909	−659	0.50	4.7330
200 m inward opening of low control roadway	7	910	−660	0.35	4.8716
	8	910	−660	0.30	5.2290
250 m inward opening of low control roadway	9	911	−661	0.30	5.0219
	10	911	−661	0.40	5.6859
300 m inward opening of low control roadway	11	913	−663	0.45	4.5965
	12	913	−663	0.40	4.3454
350 m inward opening of low control roadway	13	915	−665	0.30	5.1005
	14	915	−665	0.30	4.8301
400 m inward opening of low control roadway	15	918	−668	0.40	5.0038
	16	918	−668	0.50	4.9156
450 m inward opening of low control roadway	17	918	−668	0.30	5.2622
	18	918	−668	0.40	5.0408
500 m inward opening of low control roadway	19	920	−670	0.30	5.2569
	20	920	−670	0.35	5.1177

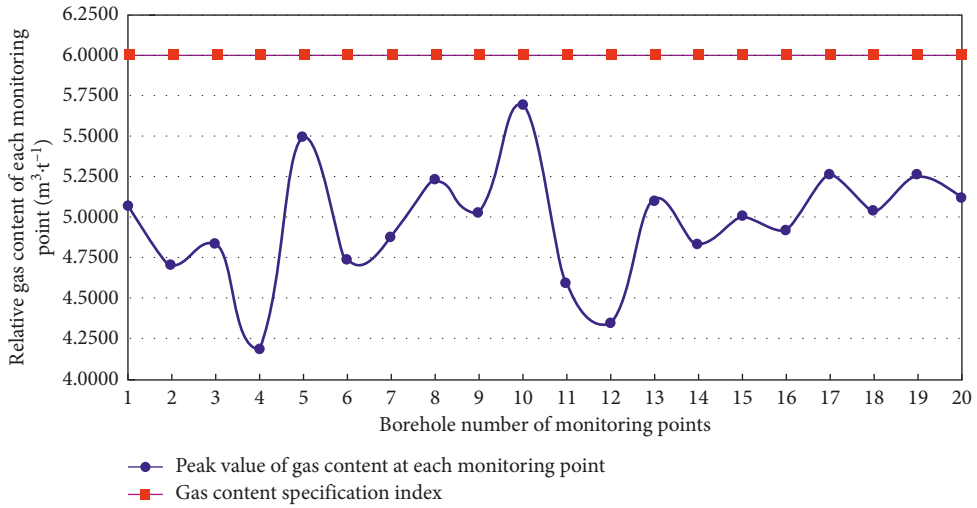

Figure 26: Gas contents of inlet lane in Panel 31020.

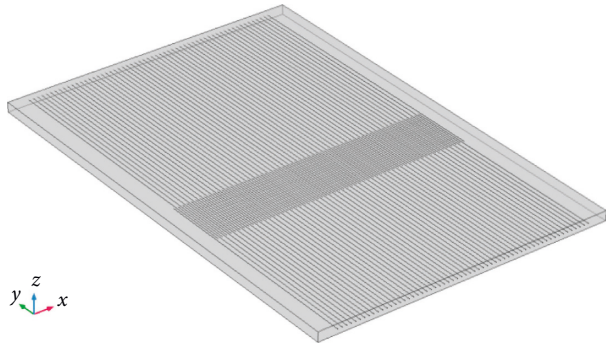

Figure 27: Geometric model of gas drainage in intake roadway of Panel 17220.

Table 5: Parameters for simulation.

Parameter	Porosity φ_0	Adsorption constant a	Adsorption constant b	Permeability k_0	Slippage factor h	Modulus of elasticity E	Poisson ratio ν
Value	0.0282	35.597 m^3/t	0.406 MPa^{-1}	0.018 mD	0.76 MPa	3.75 GPa	0.25

parameters used in the simulation are shown in Table 5. According to the stress analysis results of the Panel 17220, the stress concentration factor of the panel is 2.53. Therefore, the simulated condition is 2.53 and the extraction time is 180 days.

5.3.2. Boundary Conditions. The boundary conditions of the model are as follows: The bottom of the model is a fixed boundary, the periphery is a sliding boundary, and the boundary between coal seam and rock seam is a gas impermeable boundary. The top of the model is subjected to the gravity of the overburden rock, and the surrounding rock is subjected to the horizontal stress. The boundary of the extraction borehole is set as the Dirichlet boundary condition.

Combining with the test results of in situ stress and gas extraction, the boundary loading conditions imposed by the model are as follows: 18.25β MPa on the top of the model, 35β MPa on the lateral load in the X direction of the model, self-weight load on both coal seam and rock strata, and 41 kPa negative pressure on the boundary of the extraction borehole.

5.3.3. Analysis of Simulation Results. According to the relevant regulations of coal and gas outburst prevention and control in Henan Province, the residual gas pressure of coal seam after gas extraction should not exceed 0.6 MPa, and the residual gas content shall not exceed 6 m^3/t. Figure 28 shows the gas pressure after extraction for 180 days. When a low gas pressure area is formed near the borehole after gas extraction for 180 days, the gas pressure in the gas extraction covered area is reduced to 0.4 MPa~0.55 MPa.

5.3.4. Analysis of Simulation Results. Figure 28 shows the gas pressure after extraction for 180 days. A low gas pressure area is formed near the borehole after gas extraction for 180

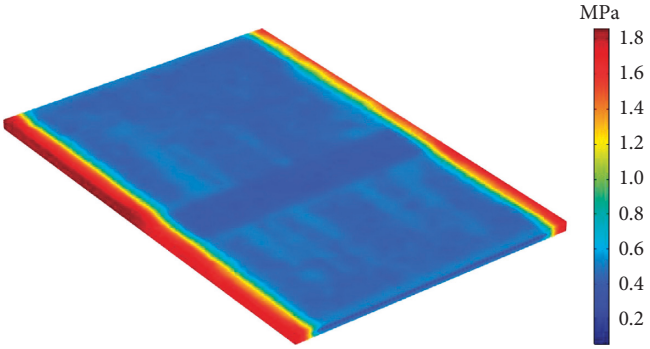

Figure 28: Gas pressure nephogram of coefficient after extraction for 180 days.

days, the gas pressure in the gas extraction covered area is reduced to 0.4 MPa~0.55 MPa.

Figure 29 shows the distribution of gas pressure in the drainage area. After 180 days of supplementary gas drainage, a distinct low-pressure area is formed in the simulated area. The gas pressure decreases to 0.1 MPa~0.42 MPa, which is 84%~96% lower than that of the original simulation scheme.

At this time, 18 peak gas pressure points are formed before and after the stress concentration outburst point, and the pressure is 0.42 MPa. Compared with the original simulation scheme, the gas pressure decreases by 96%. Gas pressure meets the relevant regulations of outburst prevention and control. The distribution curve of gas content in the drainage area is shown in Figure 30. After gas extraction for 180 days, the gas content is 5.15 m^3/t, which is 64.58% lower than that of the original simulation scheme. The gas contents meet the relevant regulations of coal and gas outburst prevention and control.

According to the simulation results, after 180 days of gas extraction, the gas pressure is 0.42 MPa, which meets the qualified index of 0.6 MPa, and the gas content is 5.15 m^3/t, which meets the qualified index of 6 m^3/t. Therefore, the gas pressure and contents after second gas

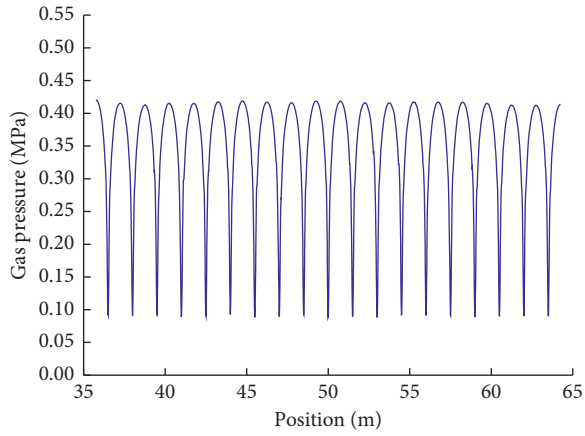

Figure 29: Distribution of gas pressure in the drainage area.

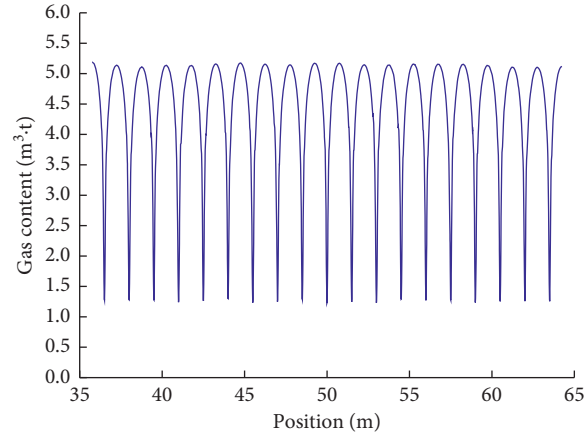

Figure 30: Distribution of gas content in the area covered by extraction.

extraction meet the relevant provisions of coal and gas outburst prevention and control, and achieve the expected effect.

6. Conclusion

Relevant factors of Panel 31020 are listed below:

(1) Panel 31020 is located in the outburst dangerous area predicted by gas geological map.

(2) Structure has a controlling effect on the occurrence of coal and rock outburst.

(3) Panel 31020 is located in normal stress area, and there is no obvious stress concentration phenomenon under natural geological conditions.

(4) The outburst risk probability of Panel 31020 is 0.95, which is high outburst risk.

(5) The stress concentration coefficient of the panel is 2.27–2.35, the stress concentration coefficient of intake roadway is 1.23–1.25, and the stress concentration coefficient of return roadway is 1.86–1.95.

(6) After second gas extraction, the gas pressure is 0.51 MPa and the gas contents is 5.14 m^3/t. The gas pressure and gas contents meet the relevant requirements of coal and gas outburst prevention and control.

A coal and gas outburst occurred on November 25th, 2017, and Panel 31020 has not being mined at present.

Relevant factors of Panel 17220 are listed below:

(1) Panel 17220 is located in the outburst dangerous area predicted by gas geological map.

(2) Structure has little effect on the occurrence of coal and rock outburst.

(3) Panel 17220 is located in normal stress area, and there is no obvious stress concentration phenomenon under natural geological conditions.

(4) The outburst risk probability of Panel 17220 is 0.90 to 0.95, which is high outburst risk.

(5) The stress concentration factor of Panel 17220 is 2.37–2.53, the stress concentration factor of intake roadway is 1.20, and the stress concentration factor of return roadway is 2.08–2.14, which increases the risk of dynamic disasters such as coal and gas outburst.

(6) After adopting the measures of gas drainage, the gas pressure value is 0.42 MPa, the gas contents value is 5.15 m^3/t, and the gas pressure and gas contents reach the coal and gas outburst prevention and control.

(7) Panel 17220 has been safely recovered.

By comparing with the correlative factors of dynamic disasters between Panel 31020 and Panel 17220, the two panels have the same results in five correlative factors, such as gas geological conditions, stress conditions, risk probability conditions, mining conditions, and risk-control measures. Only the structural conditions are different, which indicates that the structural conditions are important correlation factors to coal and gas outburst.

Nomenclature

m: Gas mass per unit volume
t: Time
∇: Hamiltonian operator
p: Gas density
u: Gas migration velocity in fissures
Q: Source term
φ: The porosity of coal body
ρ_{gs}: The gas density under standard condition
ρ_c: The density of coal
V_L: The Langmuir volume constant
P: The gas pressure of coal seam
p_L: The Langmuir pressure constant
k: The permeability of coal
μ_g: The dynamic viscosity of gas
b: The Klingberg factor
ε_{ij}: The strain of coal
σ_{ij}: The stress of coal

δ_{ij}: The Kronecker factor
G: Shear modulus of coal
D: The equivalent elastic modulus of coal
E_s: The elastic modulus of coal
L_f: The improved fracture stiffness of coal
K: The bulk modulus of coal
K_s: The bulk modulus of coal
E: The elastic modulus of coal
v: Poisson's ratio of coal
α: The Biot effective stress coefficient
ε_a: The gas adsorption strain of coal skeleton
φ_0: The initial porosity of coal
ε_L: The Langmuir strain constant
Δp: The variation of gas pressure in coal seam
k_0: The initial fracture permeability
β: The stress concentration factor.

Data Availability

The data used to support the findings of this study are available from the corresponding author upon request.

Conflicts of Interest

The authors declare that they have no conflicts of interest.

Acknowledgments

This research was financially supported by the National Natural Science Foundation of China (Grant nos. 51904145, 51674135, 51274117, and 51304110), Liaoning Natural Science Foundation Program Guidance Plan (Grant no. 2019-ZD-0045), Liaoning Provincial Department of Education Project (Grant no. LJ2019JL007), the Funds for National Standard Revision Projects of China Coal Industry Association in 2017 (Grant nos. 18-1005), and the Doctoral Research Initiation Funds of Liaoning Technical University (Grant nos. 18-1010).

References

[1] M. B. Wold, L. D. Connell, and S. K. Choi, "The role of spatial variability in coal seam parameters on gas outburst behaviour during coal mining," *International Journal of Coal Geology*, vol. 75, no. 1, pp. 1–14, 2008.

[2] H. W. Zhang and S. Li, "Pattern recognition and possibility prediction of coal and gas outburst," *Chinese Journal of Rock Mechanics and Engineering*, vol. 24, no. 19, pp. 3577–3581, 2005.

[3] B. F. Yu, "Talking about the mechanism of coal and gas outburst," *Coal Science and Technology*, vol. 8, pp. 34–42, 1979.

[4] J. Shepherd, L. K. Rixon, and L. Griffiths, "Outbursts and geological structures in coal mines: a review," *International Journal of Rock Mechanics and Mining Sciences & Geomechanics Abstracts*, vol. 18, no. 4, pp. 267–283, 1981.

[5] J. W. Yan, X. B. Zhang, and Z. M. Zhang, "Research on geological control mechanism of coal-gas outburst," *Journal of China Coal Society*, vol. 38, no. 7, pp. 1174–1178, 2013.

[6] Y. S. Zhao, "Coupled mathematical model on coal mass-methane and its numerical method," *Chinese Journal of Rock Mechanics and Engineering*, vol. 13, no. 3, pp. 229–239, 1994.

[7] Q. T. Hu, S. N. Zhou, and X. Q. Zhou, "Mechanical mechanism of coal and gas outburst process," *Journal of China Coal Society*, vol. 33, no. 12, pp. 1368–1372, 2008.

[8] F. T. Miao, D. L. Sun, and Q. T. Hu, "The formation mechanism of shock waves in the coal and gas outburst process," *Journal of China Coal Society*, vol. 38, no. 3, pp. 367–372, 2013.

[9] L. K. Zhu, H. T. Yang, T. Xu, G. H. Zhao, and Z. H. Xie, "Explore the mechanism of ground stress and gas pressure in coal-gas outburst," *Journal of Mining & Safety Engineering*, vol. 39, no. 5, pp. 1038–1044, 2018.

[10] Y. M. Yin, X. K. Zhang, F. X. Jiang, and Z. X. Yu, "Study on mechanical mechanism and danger evaluation technology of coal and gas outburst induced by rockburst," *Journal of Mining and Safety Engineering*, vol. 35, no. 4, pp. 801–809, 2018.

[11] X. Z. Chen, "Research on influence of ground stress on intensity of coal and gas outburst," *Journal of Mining & Safety Engineering, Coal Technology*, vol. 37, no. 7, pp. 159-160, 2018.

[12] C. Fan, D. Elsworth, S. Li, L. Zhou, Z. Yang, and Y. Song, "Thermo-hydro-mechanical-chemical couplings controlling CH_4 production and CO_2 sequestration in enhanced coalbed methane recovery," *Energy*, vol. 173, pp. 1054–1077, 2019.

[13] C. Fan, D. Elsworth, S. Li et al., "Modelling and optimization of enhanced coalbed methane recovery using CO2/N2 mixtures," *Fuel*, vol. 253, pp. 1114–1129, 2019.

[14] C. Fan, S. Li, M. Luo, W. Du, and Z. Yang, "Coal and gas outburst dynamic system," *International Journal of Mining Science and Technology*, vol. 27, no. 1, pp. 49–55, 2017.

[15] J. Sobczyk, "The influence of sorption processes on gas stresses leading to the coal and gas outburst in the laboratory conditions," *Fuel*, vol. 90, no. 3, pp. 1018–1023, 2011.

[16] V. Frid, "Electromagnetic radiation method for rock and gas outburst forecast," *Journal of Applied Geophysics*, vol. 38, no. 2, pp. 97–104, 1997.

[17] M. B. D. Aguado and C. G. Nicieza, "Control and prevention of gas outbursts in coal mines, Riosa–Olloniego coalfield," *International Journal of Coal Geology*, vol. 69, no. 4, pp. 253–266, 2007.

[18] D. Y. Xu, G. Q. Li, and D. Q. Li, "Study on coal and gas outburst characteristics and prevention and control measures in Xin'an coal field," *Journal of Safety Science and Technology*, vol. 12, no. 11, pp. 52–56, 2016.

[19] J. Liu, H. H. Xia, H. M. Yang, and Z. F. Wang, "Comprehensive gas prevention and control technology of fully mechanized gateway driving face in seam with coal and gas outburst," *Coal Science and Technology*, vol. 40, no. 4, pp. 67–70, 2012.

[20] J. G. Zhang, "Construction of gas prevention and control system in China Pingmei Shenma Group," *Coal Science and Technology*, vol. 45, no. 8, pp. 13–18, 2017.